Modeling and fabrication of electrically tunable quantum dot intersubband devices

Wei Wu, Dibyendu Dey, Omer G. Memis, and Hooman Mohseni[a)]
Department of Electrical Engineering and Computer Science, Bio-inspired Sensors and Optoelectronics Laboratory (BISOL), Northwestern University, Evanston, Illinois 60208, USA

(Received 28 March 2009; accepted 27 April 2009; published online 14 May 2009)

We propose an idea of forming quantum dot intersubband transition devices based on lateral electrical confinement on quantum wells. Numerical simulations show that the energy level separation in the structure can be as large as about 50 meV, and with different electric field, the energy levels can be tuned. We also demonstrate the fabrication of a large number of field-induced quantum dots by our super lens lithography technique. We achieved uniform arrays of contacts that are about 200 nm using a conventional UV source of $\lambda \sim 400$ nm. © *2009 American Institute of Physics*. [DOI: 10.1063/1.3138135]

Quantum dot has received a lot of research interests and can be applied into many different areas. For example, quantum dot intersubband optoelectronic devices, such as quantum dot infrared photodetectors (QDIPs) and quantum dot cascade lasers (QDCLs), show superior performances both theoretically and experimentally compared with the state of the art quantum well infrared photodetectors (QWIPs) and quantum well cascade lasers (QCLs).[1–7] Currently, QWIPs still require a very low operating temperature due to high thermionic emission rates and *n*-type QWIP cannot detect normal incidence radiation due to polarization selection rules,[1] and QCLs still face the limitations of fast depletion in the upper laser level by nonradiative longitudinal optical (LO)-phonon-assisted emission as well as the high optical loss.[2] However, QDIPs and QDCLs can effectively overcome those limitations because of the three-dimensional (3D) quantum confinement in the quantum dot.[2,3] To fabricate quantum dots, conventional methods include self-assembled growth,[8] lithography patterning,[9] and applying magnetic field.[10] However, it is very difficult to effectively control the size and position of the quantum dots by the self-assembled growth. Lithography method always produces defects on the etched surfaces and is too slow and expensive to produce a large amount of quantum dots, and the magnetic field method requires a large setup for generating the required high magnetic field.

Here we propose a method of applying a lateral external electrical field on quantum wells to produce 3D quantum confinement.[11] The lateral field applied results in a lateral energy confinement that breaks the in-plane periodic potentials and hence collapses the energy bands in the quantum well into energy states. The lateral quantum confinement can be tuned by the electric field. The energy states will shift toward higher energy values with a higher lateral electric field. Unlike the lateral quantum confinements based on material-wet or -dry etchings the method proposed here is defect-free and field-induced, and therefore it is easily tuned and the dot sizes can be more uniform. Our self-assembled nanolithography technique, called super lens lithography (SLL),[12,13] has been applied to produce a large area of highly uniform quantum dots. A thickness controllable electrical anodization method[14] has been used to grow an electrically insulated layer to separate the top and gate contacts for all the dots. Besides, six photolithography steps have been used to produce and separate different contact layers of the devices. The processing can be applied into both field-induced QDIPs and QDCLs. The processing steps and conditions may also be used to fabricate other similar electronic and optoelectronic devices.

To apply a lateral field on quantum well layers we designed a device structure shown in Fig. 1(a). In the structure, gate contact, the insulator below the gate and semiconductor quantum well layers form a metal-insulator-semiconductor structure. When applying a negative voltage on gate contact and a positive one on top injector, a lateral electrical field is induced, by which it depletes electrons under the gate and confine them into the nanochannel below the top injector. The diameter of a top injector is about 200 nm. Between the gate and top injector contacts, there is an insulation layer formed by electrical anodization, which isolates the two contacts. The top injector is contacting with the top surface of the semiconductor layers. A back contact is also formed. All the gates are connected to each other.

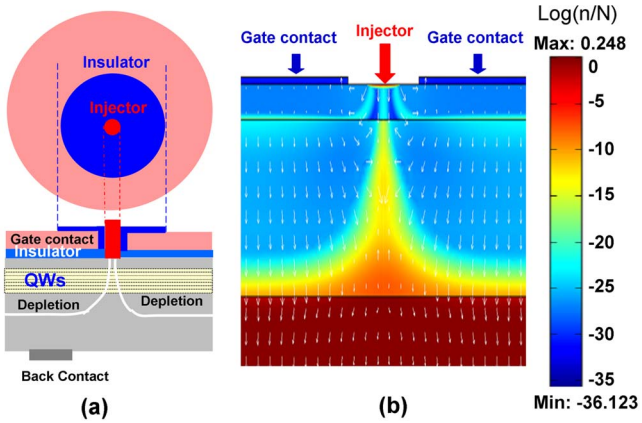

FIG. 1. (Color online) (a) schematic diagram of an electrically tunable quantum dot device (the white dashed lines are the isopotential lines, and the electrons are depleted into the nanochannel below the injector); and (b) 3D FEM simulation of electron depletion into the nanochannel below the injector (n is the electron concentration and N is the average doping concentration of quantum well layers).

[a)]Electronic mail: hmohseni@northwestern.edu.

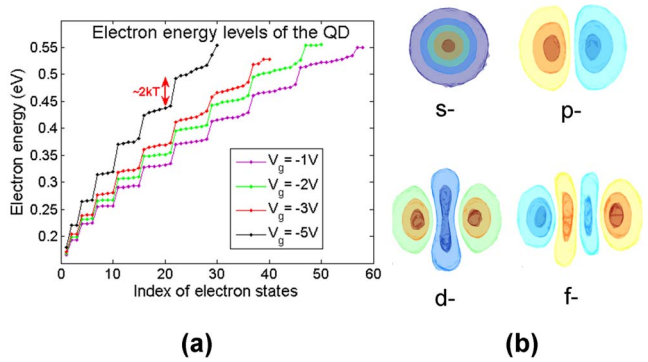

FIG. 2. (Color online) (a) Electron energy level of a single quantum well after lateral electron confinement with different gate voltages; and (b) typical wave functions calculated inside the quantum dot.

We used 3D finite-element-method (FEM) simulation to calculate the confinement of electrons in the nanochannel below the injector shown in Fig. 1(b). The voltage applied on the gate contact was −4.5 V and the voltage on the top contact was 4.5 V. The top contact layer was 100 nm InGaAs with a donor doping density of 3×10^{16} cm^{-3}. The quantum well active layers consisting of InGaAs and InAlAs had the thickness of 500 nm with an average donor doping density of 3.5×10^{16} cm^{-3}, and the bottom layer was InP substrate. With different gate voltages, different depletion widths in the quantum wells were formed and thus the QD size is effectively changed. In Fig. 2(a) using 3D FEM simulations we found that the electron energies were shifted to higher values with a more negative gate voltage and the separation between two adjacent energy levels at −4.5 V for gate voltage reached ~50 meV, while the LO phonon energy is typically <40 meV.[15] Thus the conservation of energy cannot be satisfied with the emission of a single of LO phonon. This effectively reduces the nonradiative electron-phonon scattering, which could greatly increase the gain values of photodetectors and reduce the nonradiative loss of infrared lasers. The typical electron wave functions, such as the *s*-, *p*-, *d*-, and *f*-like wave functions, were also calculated [see Fig. 2(b)].

We started our processing from a QWIP or QCL wafer sample. Six photolithography masks were used. The sample was deposited with a high quality film of SiO_2 by plasma enhanced chemical vapor deposition. The SiO_2 layer was used as the insulator between the gate and semiconductor layers. After deposition, the sample was patterned with the gate contacts consisting of Ti/Au pad and a thick Al layer. The SLL technique was applied to produce a large area of uniform nanoholes (diameter of ~200 nm) in a thin Al film. Figure 3(a) shows the top view of the sample covered with a large area of uniform nanoholes in the Al film and the gate contact, and Fig. 3(b) is the enlarged view of the nanoholes, each of which producing a quantum dot. A controllable electrical anodization method[14] was applied to anodize the surface of the aluminum layer perforated with nanoholes and generate the insulator, aluminum oxide, which was between the top and gate contact layers. The thickness of the insulator was controlled with a final anodization voltage, and it showed a very low leakage current density with a high breakdown voltage. After anodization, reactive ion etching (RIE) method was used to anisotropically etch the dielectric SiO_2 layer inside the nanoholes. A ratio of 9:1 gases of CF_4 and

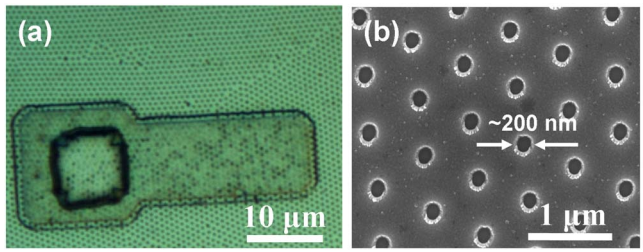

FIG. 3. (Color online) (a) The top view of the sample after generating a large area of uniform nanoholes perforated in Al layer and gate contact; and (b) the zoomed in view of the nanoholes perforated in Al layer.

O_2 under the pressure of 75 mTorr and the plasma power of 60 W were found to give a good sidewall etching of the SiO_2 layer with etching rate of ~20 nm/min, while not etching the anodized Al layer. After plasma-etching the SiO_2 layer in the nanoholes, a top Ti/Au layer was deposited to fill the nanoholes using electron-beam evaporation and patterned by photolithography. To fully fill these tiny holes and avoid a bad contact, the sample needs to be rotated while deposition. Figure 4(a) shows the side view of the nanoholes filled with Ti/Au top injector layers and Fig. 4(b) is the enlarged view of a single nanohole with the top injector. The structure in Fig. 1(a) has been formed. After patterning the top contact patterns, to fabricate QDIPs or QDCLs we deposited another thick SiO_2 layer and patterned it as a mesa or ridge using photolithography. The mesa/ridge was used as a mask to wet-etch the semiconductor layers below and form a pixel in QDIPs or a ridge cavity in QDCLs, the same as the standard processing steps in QWIPs or QCLs. After etching the semiconductors, SiN was deposited to passivate the semiconductor surface. The SiN layer was opened using photolithography patterning and RIE etching, and Ti/Au metal layers were deposited to produce contacts. Finally, a separation photolithography mask was used to separate the top and gate contact layers.

We have outlined the basic idea and motivation in forming tunable quantum dot intersubband device based on lateral electrical confinement on quantum wells. The method of forming quantum dot by electrical confinement effectively avoids the surface defect states introduced in the etching-based method and generates much more uniform quantum dots compared with the strain-induced growth method. The preliminary fabrication success has been described. The method of fabricating quantum dots described here is a self-aligned and self-isolated process. It eliminates the difficulties of alignment of submicron process and effectively avoids the short circuits for all the devices. All the patterning used in the process is solely based on conventional UV photolithography. Further experiments such as intersubband spectroscopy and magnetotransport measurement can be used to

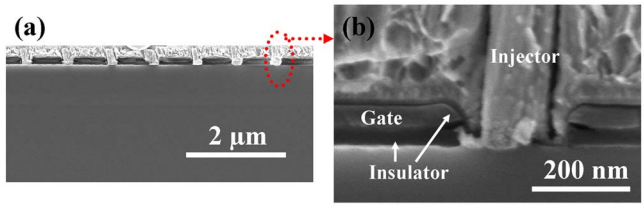

FIG. 4. (Color online) (a) Side view of the nanoholes filled with Ti/Au top injector; and (b) the zoomed in view of a single quantum dot.

prove the existence of bound states in the quantum dots and further characterizations of electrically confined QDCL are under investigation.

This work was partially supported by the National Science Foundation under Grant No. ECCS-0621887 and the Defense Advanced Research Project Agency under Grant No. N00014-07-1-0564.

[1]J. C. Campbell and A. Madhukar, Proc. IEEE **95**, 1815 (2007).
[2]I. A. Dmitriev and R. A. Suris, Physica E (Amsterdam) **40**, 2007 (2008).
[3]S. Kim, H. Mohseni, M. Erdtmann, E. Michel, C. Jelen, and M. Razeghi, Appl. Phys. Lett. **73**, 963 (1998).
[4]N. S. Wingreen and C. A. Stafford, IEEE J. Quantum Electron. **33**, 1170 (1997).
[5]J. Phillips, J. Appl. Phys. **91**, 4590 (2002).
[6]D. Pan, E. Towe, and S. Kennerly, Appl. Phys. Lett. **73**, 1937 (1998).
[7]L. Chu, M. Arzberger, A. Zrenner, G. Bohm, and G. Abstreiter, Appl. Phys. Lett. **75**, 2247 (1999).
[8]J. Urayama, T. B. Norris, J. Singh, and P. Bhattacharya, Phys. Rev. Lett. **86**, 4930 (2001).
[9]K. H. Wang, A. Pecher, E. Hofling, and A. Forchel, J. Vac. Sci. Technol. B **15**, 2829 (1997).
[10]C. Becker, C. Sirtori, O. Drachenko, V. Rylkov, D. Smirnov, and J. Leotin, Appl. Phys. Lett. **81**, 2941 (2002).
[11]H. Mohseni and W. Chan, U.S. Patent No. 7026641 (April 11, 2006).
[12]W. Wu, D. Dey, A. Katsnelson, O. G. Memis, and H. Mohseni, J. Vac. Sci. Technol. B **26**, 1745 (2008).
[13]W. Wu, A. Katsnelson, O. Memis, and H. Mohseni, Nanotechnology **18**, 485302 (2007).
[14]T. W. Hickmott, J. Appl. Phys. **87**, 7903 (2000).
[15]P. Bhattacharya, K. K. Kamath, J. Singh, D. Klotzkin, J. Phillips, H. Jiang, N. Chervela, T. B. Norris, T. Sosnowski, J. Laskar, and M. R. Murty, IEEE Trans. Electron Devices **46**, 871 (1999).